View metadata, citation and similar papers at core.ac.uk
brought to you by CORE
provided by Elsevier - Publisher Connector

Biochimica et Biophysica Acta 1828 (2013) 2272–2282

Contents lists available at SciVerse ScienceDirect

Biochimica et Biophysica Acta

journal homepage: www.elsevier.com/locate/bbamem

Review

# Super-resolved FT-IR spectroscopy: Strategies, challenges, and opportunities for membrane biophysics ☆

Jessica J. Li [b], Christopher M. Yip [a,b,*]

[a] Institute of Biomaterials and Biomedical Engineering, University of Toronto, Toronto, CanadaM5S 3E1
[b] Department of Chemical Engineering and Applied Chemistry, Terrence Donnelly Centre for Cellular and Biomolecular Research, University of Toronto, Toronto, Canada M5S 3E1

A R T I C L E I N F O

*Article history:*
Received 16 December 2012
Accepted 25 February 2013
Available online 13 March 2013

*Keywords:*
Infrared
Spectroscopy
Scanning
Probe
Microscopy

A B S T R A C T

Direct correlation of molecular conformation with local structure is critical to studies of protein– and peptide–membrane interactions, particularly in the context of membrane-facilitated aggregation, and disruption or disordering. Infrared spectroscopy has long been a mainstay for determining molecular conformation, following folding dynamics, and characterizing reactions. While tremendous advances have been made in improving the spectral and temporal resolution of infrared spectroscopy, it has only been with the introduction of scanned-probe techniques that exploit the raster-scanning tip as either a source, scattering tool, or measurement probe that researchers have been able to obtain sub-diffraction limit IR spectra. This review will examine the history of correlated scanned-probe IR spectroscopies, from their inception to their use in studies of molecular aggregates, membrane domains, and cellular structures. The challenges and opportunities that these platforms present for examining dynamic phenomena will be discussed. This article is part of a Special Issue entitled: FTIR in membrane proteins and peptide studies.

© 2013 Elsevier B.V. All rights reserved.

**Contents**

1. Introduction . . . 2272
2. Coupled ATR-IR and SPM . . . 2273
3. Near-field scanning infrared microscopy . . . 2274
4. AFMIR–photothermal induced resonance (PTIR) . . . 2276
5. Summary . . . 2278
References . . . 2278

## 1. Introduction

Recent advances in high-resolution correlated imaging tools have provided tremendous new insights into protein structure, dynamics, and interactions, often in real-time, and under physiologically relevant conditions. These efforts have gained significant impetus through the introduction, development, and now optimization of super-resolution optical techniques such as STORM, STED, PALM, FIONA, among others [1–13]. These approaches build on innovative strategies related to fluorophore design, illumination strategies, and post-acquisition image analysis and processing, as in the case of SOFI and fluctuation analysis [14–18]. The net result of these advances has been a suite of platforms that enable optical resolution well beyond the conventional far-field diffraction limit and depending on the technique can achieve localization precision to within a few nanometers.

However, there remain numerous key challenges and caveats underscoring these admittedly powerful strategies, including selection of a fluorophore with appropriate excitation and emission characteristics, photobleaching and other photophysical effects, and in the case of extrinsic labeling, considerations of the effect of site mutation on native conformation, interactions, and dynamics. Indeed, the addition of an extrinsic fluorophore has been shown to dramatically influence the spatial distribution of membrane-associated proteins [19]. Such effects have certainly driven interest in the use of combinatorial tools and techniques that enable simultaneous acquisition of multi-parameter data, ideally on the same length scale. These include coupled and correlated optical-scanning probe microscopy (SPM) [20–32]. These approaches allow one to map structural changes with specific molecular phenomena, such as domain localization and restructuring

☆ This article is part of a Special Issue entitled: FTIR in membrane proteins and peptide studies.

* Corresponding author. Tel.: +1 416 978 7853; fax: +1 416 978 4317.
*E-mail address:* christopher.yip@utoronto.ca (C.M. Yip).

0005-2736/$ – see front matter © 2013 Elsevier B.V. All rights reserved.
http://dx.doi.org/10.1016/j.bbamem.2013.02.013

[33], while we and others used this strategy to follow enzymatic processes at membrane surfaces [20,21,34,35]. Fluorescence-based approaches have certainly been used successfully to interrogate changes in molecular conformation, lipid-induced secondary structure changes and/or alterations to lipid structure or packing. However, these are largely indirect strategies requiring careful provisioning of appropriate controls and consideration of many of the key points described above. This is particularly true in the case of using extrinsic dyes to report on local changes to domain structure or lipid structure and chemistry where it has been shown that reliance on fluorescence alone can lead to erroneous conclusions regarding lipid domain composition and interactions [19]. Correlated fluorescence-SPM approaches are particularly well-suited for examining protein aggregates and fibrils, including membrane-induced nucleation and growth, often in the context of diseases such as Parkinson's, and Alzheimer's. However, often these approaches rely on binding of extrinsic dyes, such as Congo Red or thiaflavin T, and changes in their emission characteristics or photophysical behavior in order to provide insights into their local environment and by extension, changes in the protein's secondary structure [36–40].

In contrast, infrared spectroscopy does not rely on an extrinsic label and can provide direct insights into local secondary structure. Its potential for tracking protein and peptide conformation and aggregation is well known [41–44], with recent advances in two-dimensional and ultra-fast approaches heralding a new generation of IR tools for biophysicists [45–52]. A particularly useful technique for examining peptide–membrane interactions, lipid dynamics, and membrane protein conformation is attenuated total reflection infrared spectroscopy (ATR-IR) [53,54]. Studies of membrane-associated [55–58] and membranolytic peptides [59–64], along with fusion peptides and transmembrane proteins [65–67] clearly illustrate the power of this in situ approach. Polarized ATR-IR has proven to be a powerful means of investigating, for instance, electric field-induced reorientation of lipid headgroups [68], the role of lipid type on the conformation of transmembrane receptors [69,70], insulin fibril formation [71], protein association with lipid bilayers [72], lipid bilayer formation [73,74], protein orientation at solid surfaces [75], and peptide–lipid interactions [76–83]. Related to this approach for characterizing protein–membrane interactions are reflectance-absorbance strategies (IRRAS), including polarization modulation (PM-IRRAS), as exemplified by the outstanding work of the Mendelsohn and Lipkowski labs, among others [72,84–96]. Providing a two-dimensional map of spectral intensity, conventional far-field FT-IR microscopy is a particularly powerful approach for providing spatially resolved spectra of surfaces, structures, and more recently, tissues, tumors, and single cells [97–106]. With the advent of focal-plane detection, stronger light sources, and innovative approaches for post-acquisition data analysis and processing, significant strides have been made to improve the spatial and temporal resolution, and scope of application for IR microspectroscopy [106–112].

However, as in the case of conventional fluorescence microscopy, far-field FT-IR microscopy remains diffraction-limited and it was arguably with the introduction of scanned probe microscopy that the opportunity of acquiring super-resolved IR spectra arose. In scanning probe microscopy (SPM), interactions between a raster-scanning sharp tip and a surface of interest are used to generate interaction surface maps with nanometer-scale resolution. The power of this tool lies in its ability to acquire these images under a wide range of operating conditions. Numerous reviews have detailed the capabilities of this platform technique for examining biological samples and in particular membrane dynamics and structures with near-molecular scale spatial resolution [113–118]. There remains however a fundamental challenge with SPM-based imaging, namely that conclusions are inferred from morphological or topographical features. It is conventionally very difficult to use SPM to confirm specific molecular conformation, especially in the case of protein–membrane interactions. In this case, a protein may undergo subtle conformational changes upon insertion in the membrane that may be critical to its function. SPM lacks the ability to directly measure such conformational changes and can, arguably, only resolve features that are topographically distinct. This has led to a surge of interest in the development of hybrid SPM platforms that integrate other spectroscopic and characterization approaches. These include the aforementioned optical spectroscopies along with electrochemical and ion conductance measurement modalities [30,119–121].

Given the relative ease with which the SPM can be integrated with complementary techniques, it would seem reasonable to consider a hybrid of vibrational spectroscopy and SPM. Such a system would provide a compelling approach for tracking, simultaneously, conformational changes, not resolvable by in situ SPM, with topographical details that are not readily identified by conventional diffraction-limited vibrational spectroscopy. It will facilitate investigations into the relationship between physical shape and size and functional activity of integral membrane and membrane-associated protein complexes. Coupling these two techniques so that they can be applied simultaneously could in principle allow one to investigate [1] how protein assembly at the surface of a cell-mimicking lipid bilayer is facilitated by changes in molecular conformation; [2] how changes in lipid membrane surface topography, induced by pH, temperature, or soluble factors, can be directly correlated with changes in lipid conformation and packing; [3] how binding of a soluble ligand to a transmembrane receptor, as determined by changes in the shape/size/orientation of the ligand–receptor complex, result in conformational changes in the membrane receptor that are consistent with its activation; [4] how the morphology – linear fibers/helical fibers/sheets/amorphous “blobs” – of protein aggregates correlates with specific molecular conformations. This would represent a powerful platform for investigating protein–protein, protein–lipid, and protein–surface interactions that combines the spatial resolution of SPM with the spectral information available from infrared spectroscopy. In principle, there are several approaches for integrating vibrational spectroscopy with SPM, each presenting its own set of advantages, potential scope of use, and challenges. These will each be described in turn, exploring the potential advantages and disadvantages of each approach, and their relative ease of implementation.

## 2. Coupled ATR-IR and SPM

In what is likely the most straightforward implementation, hybrid infrared spectroscopy–SPM platforms have been constructed by a number of groups by simply physically mating the SPM scanner with an ATR crystal holder thereby enabling simultaneous acquisition of topographic details by SPM and infrared absorption spectra by ATR [122,123] (Fig. 1). This is a particularly convenient physical configuration since the ATR crystal serves as both the sample support and the spectral sensing element [123,124]. All of the key advantages of ATR spectroscopy are retained, including the ability to characterize samples in fluid, which is critical for biophysical research, while retaining the SPM's ability to acquire nanometer-scale topographical data of adsorbed materials on the ATR crystal itself. As was demonstrated in the work by both the Mizakoff and Yip labs, this platform is very well-suited for studying phase transitions in materials adsorbed, or grown, on the ATR crystal surface. Uniquely, the SPM provides detailed insights into conformational changes in the absorbed molecules, and also resolves structural differences in the absorbed molecules.

Since this is simply a physical marriage of the two platforms, the IR spectra are necessarily collected over a large area and the tacit assumption is made that the SPM image and IR spectra are spatially correlated. While this may generally be reasonable, there are certainly numerous examples where the scanning action of the SPM tip serves to enhance convective mass transfer into (or out of) the imaging field of view. Whether this is manifested in the IR spectra would be difficult to assess, especially since the SPM field of view comprises such

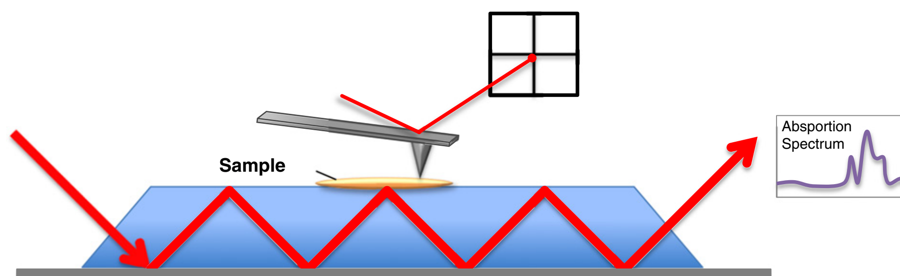


**Fig. 1.** Schematic representation of coupled ATR-IR with SPM.

a small portion of the IR sampling window in the context of a multi-bounce ATR internal reflection element. Possible approaches to alleviate these concerns include using a single bounce ATR element and/or sampling multiple regions of interest within the sampling area of the IR beam itself. Another key consideration for this ATR-based approach is the necessity of using an IR-transmissive substrate as the support. This is conventionally Ge, ZnSe, or Si, although diamond has also been used successfully. Since the sample necessarily needs to be in physical contact with the ATR crystal itself, the sample's interactions with the crystal itself need to be carefully considered. These include the available spectral window as well as the effect of surface roughness and/or chemistry on the absorbed species. It is certainly well appreciated by surface chemistry and/or structure can dramatically affect the orientation, conformation, and indeed assembly of proteins and peptides [125]. Indeed, the ease of forming a coherent intact supported lipid bilayer on an ATR crystal can be both lipid- and ATR crystal-dependent [123,126].

## 3. Near-field scanning infrared microscopy

Alternatively, confining the IR sampling to the region immediately under the scanning SPM tip by either using the tip as the source or detector would provide spatially correlated SPM and IR spectra. This concept of near-field vibrational spectroscopy was first reported by Knoll and Keilman and others over a decade ago [124,127–134]. Based on scattering of infrared radiation by a metal-coated SPM tip as it scans over a surface, the primary application of near-field vibrational microscopy has been for chemical mapping studies of thin films. While the original work by Knoll and Keilman illustrated the use of this approach for examining physical blends of immiscible polymers (PS/PMMA) [135], recently, Mueller and others studied phase separation in PS–PMMA diblock-copolymer thin films using ANSIM (Apertureless Near-field Scanning Infrared Microscopy) [136] building on earlier work by Akhremitchev, Pollack, and Walker [137–139]. Remarkably, they were able to demonstrate spatial resolution of the spectral signal well below the diffraction limit. This work is particularly notable as it not only demonstrated proof-of-concept for the application of ANSIM but also provided a compelling set of models to explain the basis for the infrared contrast mechanism, including the effect of topography (Fig. 2).

This latter component is particularly important since the tip is simultaneously acting as the infrared radiation scattering center and providing topographical contrast. By implementing an innovative homodyne referencing scheme, the authors' ANSIM approach compensates for the effect of topography thus allowing the SPM topography and near-field infrared signals to be acquired simultaneously. This is notable since many of the correlated tip-based strategies, such as magnetic and electric force microscopy, often require an interleaved scanning strategy. This approach typically involves a first-pass scan to acquire a topographical data set followed by a repeat scan with the SPM tip “lifted” a few nanometers away from the surface. During the repeat scan, changes in the cantilever's resonant frequency are plotted as a function of x–y position and then correlated against the topographical signal [140–142].

Romanov and Walker elegantly demonstrated the high spatial and spectral resolution of ANSIM in their study of di-iron nanocarbonyl particles wherein they realized single vibrational mode resolution of isolated aggregates on gold [143]. Interestingly, they found that the near-field scattering spectra were shifted in wavelength relative to the conventional far-field IR spectra and that these shifts could be reasonably explained by an angular dependence and phase shift of the back-scattered signal. While this close correspondence was taken as proof that the ANSIM strategy is capable of acquiring high spatially resolved chemical information, it remained unclear as to whether the lateral resolution reflected inter-particle/inter-aggregate spacing or an isolated individual particle. This was further complicated by the observation that the near-field IR scattering signal was found to be feature height-dependent, consistent with the general premise that for these near-field systems, the spatial resolution was highly dependent on the size and shape of the object in question. These approaches are clearly critically dependent on the actual physical size, shape, and aspect ratio of the SPM tip itself; however, the model representations tacitly assume a spherically symmetric scattering center. This certainly raises the question regarding the models themselves are sufficiently robust to account for deviations from an ideal scattering center or whether other correction factors may be required to more accurately model the ensuing near-field IR spectra. Nevertheless, this work

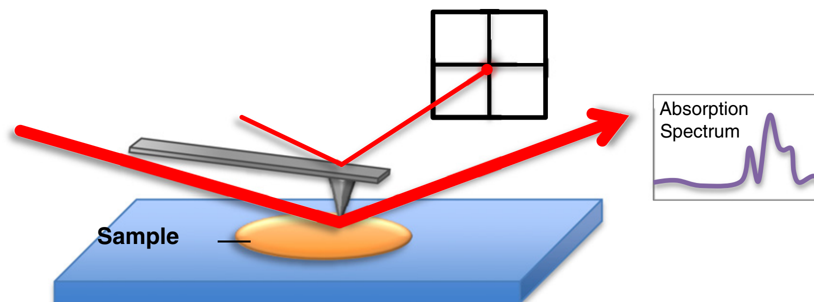


**Fig. 2.** Schematic representation of ANSIM platform.

provides provocative support of the potential of ANSIM for super-resolved chemical mapping by infrared spectroscopy.

While its potential is clear for polymer thin films and materials science applications, to date, the applications of ANSIM in biology and biophysics have been limited. Recently, Paulite et al. applied ANSIM to examine the secondary structure of β2-microglobulin fibrils [144]. This is a particularly exciting report since the direct characterization of protein aggregation and specifically, the role of conformational changes in nucleation and growth has tremendous implications for the studies of diseases such as diabetes, Alzheimer's, and Parkinson's for which protein misfolding and fibril formation are key hallmarks. While there have been extensive studies of these self-assembly and misfolding processes by in situ SPM, fluorescence spectroscopy and microscopy, solid-state NMR, and indeed conventional infrared spectroscopy [145–165], these approaches are challenged by the inability to directly correlate morphological details, as determined by techniques such as SPM, with secondary structure changes, as may be resolved by the other spectroscopic approaches. In many cases, indirect inferences are made regarding the local structure and conformation of the fibrils, including the potential of polymorphism. This is further complicated by keen interest in the dynamics of aggregate formation and the role of substrates or initiators in facilitating conformational changes associated with fibril or oligomer nucleation. Studies of these assembly pathways would be substantially enhanced if it were possible to directly image individual protein aggregates and directly correlate morphologies with secondary structure, including the critical size and/or local environments associated with specific conformational states [165]. In their work, Paulite et al. applied ANSIM to study mature β2-microglobulin fibrils, obtaining remarkable ~30 nm spatially resolved IR spectra. What was quite compelling about this work was the good correspondence between the experimentally measured near field IR signal and the calculated scattering signal based on a far-field IR absorption spectrum using a coupled dipoles model. Notably, the authors also interpreted the intensity of specific spectral features in terms of the fibril twist angle and the polarization of the IR laser, in effect mapping fibril orientation on the substrate. This is a powerful demonstration of the ability of IR spectroscopy in general to provide insights into molecular conformation and orientation at surfaces when polarization is taken into account. Furthermore, in this particular context, resolving individual fibril twist and orientation both topographically and spectroscopically portends the use of ANSIM for tracking more complex aggregation phenomena. Despite these encouraging results, it is worth noting that this effort was directed at mapping changes in the Amide I 1600–1700 $cm^{-1}$ wavenumber range and specifically β-sheet content, and while in principle there is no reason to not be examining other regions of the mid-IR, there are several practical considerations that need to be reconciled.

Since ANSIM relies on near-field scattering of a tunable IR laser, repeat imaging must be performed at each wavelength of interest in order to generate a reasonable approximation of the absorbance spectrum for each location in the field of view. This would suggest that acquiring spectra with sub-wavenumber resolution, as would be commonly obtained using conventional far field approaches, would be a time-intensive process and indeed, the authors only provided data for a few selected wavenumbers. This also raises the rather vexing issue of examining dynamic phenomena using this approach. Clearly understanding aggregation requires that one be able to probe the dynamic events associated with nucleation and growth, including putative conformational changes, as may be the case when a soluble protein associates with a surface or membrane and then undergoes a secondary structure change that encourages fibril growth. Such dynamics have certainly been probed using tools such as stopped-flow fluorescence, circular dichroism, and time-resolved infrared spectroscopy [157,166–169]. It remains unclear as to whether the ANSIM approach would be, at present, capable of resolving fast dynamics.

A recent report by Huth et al., described the use of a coherent continuum source based on the super-position of two femto-second near-infrared laser pulses in a Michelson interferometer geometry [170]. Unlike the tunable approach described previously, this strategy provides a continuous source that spans the so-called molecular fingerprint range of 700–2100 $cm^{-1}$ yielding excellent agreement between the near-field scattering and conventional far-field FT-IR absorption spectra. In this proof-of-concept effort, they were able to provide 20 nm spatially resolved spectra of 90 nm thick films of PMMA on Si wherein the spatial resolution was solely determined by the radius of the scanning tip with spectral acquisition times and resolution comparable to that for conventional FT-IR. While the authors provided a strong theoretical basis for this agreement, their model assumptions included a spectrally flat background and no tip-induced resonances.

While these technical implementations do certainly represent a critical advance for the field of super-resolution IR spectroscopy, and the inherent potential for examining structures such as protein aggregates and fibrils is significant, a number of key questions regarding the use of tip-scattering near-field approaches for biophysical research remain. These include whether they are appropriate for use in fluid as the acquisition of IR spectra in fluid would certainly yield more relevant insights into the effect of pH and soluble agents, and whether it will be possible to directly interrogate the dynamics of protein– and peptide–membrane interactions, rather than simply ex situ, post-facto analysis of individual structures.

In a related approach, a number of groups have advanced the concept of near field scanning optical microscopy using an IR source (IR-Scanning Near-Field Optical Microscopy: IR-SNOM). This platform uses an IR-compatible optical fiber tip in place of a conventional SPM tip [171]. The tip is raster-scanned over a surface that is illuminated by an IR beam, either separately, or through the optical fiber itself. Measuring the IR light that is reflected back into the optical fiber can then be used to create an IR absorbance map of the surface. In direct analogy to the ANSIM approach, a spectrally resolved image would be generated by sequentially illuminating the sample with the IR wavelength of interest. Unlike the ANSIM approach however, which uses the conventional deflection feedback mechanism for the SPM, in the SNOM strategy, the topographical data are collected using a shear-force feedback scheme. Building off proof-of-concept work in the materials and polymer science field [172–174], the Piston group at Vanderbilt has demonstrated the feasibility of this approach for chemically mapping cells in fluid [175,176]. This work was quickly followed by tantalizing images of lipid multilayers on gold substrates wherein images acquired at specific IR wavelengths revealed structural details ascribed to local order and clustering [177,178]. Interestingly, the images revealed regions that could be identified as having strong $-CH_2-$ and $PO_2^-$ absorbances that were, for the most part, spatially correlated. This would certainly seem reasonable since the spatial resolution of this aperture-based approach is ~100 nm, which, while below the diffraction limit, would not be sufficient to distinguish any in-plane shift of the lipid headgroups relative to their tails. In a rather interesting correlative study, Generosi and others used IR-SNOM to identify receptor clusters in neuronal cells [179,180]. By labeling the AMPA receptor with the extrinsic fluorophore Alexa-488, they were able to identify clusters on the surface of the cells that bore the unique IR signature of the fluorophore. Remarkably they were able to demonstrate localization of the dye's unique IR signature to specific regions of the neuronal cells with a lateral resolution of ~350 nm. Although ideally, one would rather not have to rely on extrinsic probes, this does provide a unique opportunity of performing a multimodal correlated fluorescence-IR–SPM imaging experiment on live cells. It is worth noting that unlike the ANSIM approach, the SNOM strategy is perhaps better suited for imaging in fluid media; however, it is clear that it cannot provide comparable spatial resolution to the scattering-based approaches such as ANSIM. It does share

the same challenges as ANSIM in terms of acquisition times, tip shape and characteristics, and the need for repeat scans at each wavelength of interest, which could be particularly challenging for probing real-time phenomena. Indeed, most of the cell work by SNOM-IR has been performed on fixed, rather than live cells.

## 4. AFMIR–photothermal induced resonance (PTIR)

Thus far, we have considered two approaches that considered the integration of scanning probe microscopy with FT-IR spectroscopy. The first, which integrated a scanned probe microscope with a conventional ATR-FTIR platform, does not afford super-resolved IR spectra but does enable imaging and spectral acquisition in fluid media. The second enables super-resolved spectroscopy with simultaneous acquisition of topographical data on the nanometer length scale using a near-field tip-based scattering strategy. Complementing these approaches, Dazzi et al., recently introduced a new SPM-based approach for super-resolved IR spectroscopy that exploits a photothermal acoustic effect for chemical mapping [181–183]. In this strategy termed AFMIR (or photothermal induced resonance (PTIR)), a sample mounted on a ZnSe crystal is illuminated by a pulse of infrared light while being imaged by the SPM in contact mode (Fig. 3).

The orientation is such that the IR pulse is directed in a total internal reflection geometry within the ZnSe crystal itself. Absorption of ps pulses of infrared light by the sample results in a thermal–mechanical expansion of the sample, which in turn induces a transient excitation of the SPM tip. By sampling a range of spectral wavelengths, an absorption spectrum can then be recreated from an FFT analysis of the cantilever tip's response. Remarkably, the authors were able to theoretically demonstrate that this effect is due not to the actual thermal expansion of the sample, associated with absorption of specific IR wavelengths, but rather the expansion rate [184]. As in the case of ANSIM, the initial proof of concept studies emphasized the application of PTIR for materials science applications with a dramatic illustration of its potential in mapping of an individual, isolated semiconductor quantum dot buried within a host matrix [185]. Using a 200 nm Au-coated SPM tip operating in contact, the authors were able to acquire mid-IR spectra of n-doped InAs/GaAs with ~λ/150 nm spatial resolution using an excitation wavelength of ~9.6 μm. Despite challenges associated with slight shifts in the apparent spectra that were attributed to topographical roughness and doping levels, this work was certainly encouraging and has led to in-depth investigations into not only potential applications of PTIR, including its suitability for examining polymer blends but also the underlying technical challenges and opportunities [186–189].

Since the SPM tip is serving as the IR detector in the PTIR platform, understanding how to best optimize its response to the PT signal has been a key priority. In recent work, Kjoller et al., examined how changes to the SPM cantilever itself can result in improved response, sensitivity, and resolution [190]. As with all spectroscopic approaches, improving signal to noise necessitates co-averaging a large number of scans. In the case of the PTIR approach, as opposed to conventional far-field IR, this can result in a reduction in the spatial resolution of the technique itself as sample heating can become a significant issue upon repeated IR pulses. By redesigning the SPM cantilever itself so that it retains its topographical sensitivity, the authors were able to improve the signal to noise ratio and significantly reduce the time required to acquire a spectrum by almost an order of magnitude. This creative approach involved physically etching away part of the cantilever itself to create what the authors describe as “an internal paddle”. This mechanical alteration changes the vibrational characteristics of the cantilever, resulting in an extended temporal response to the ps excitation IR pulse, and a concomitant improvement in the cantilever's quality factor. This is a remarkably innovative approach that does not appear to compromise the SPM's ability to provide high spatial (topographical) resolution.

While these technical advances are certainly encouraging for the future of PTIR, a number of underlying questions or considerations remain. These include the thermal conductivity and diffusivity of the sample or materials under study, the presence of phase or domain boundaries, and the degree of structural/chemical heterogeneity, all of which could conspire to affect the spatial resolution of the PTIR spectra. Recent work by Felts et al., has started to address some of the questions in their study of thermoplastic nanostructures created by tip-based deposition [191]. Using the SPM tip as a fabrication tool, well-defined lines of PE (polyethylene), PS (polystyrene) and PDDT (poly(3-dodecylthiophene-2,5-diyl)) were patterned onto the ZnSe prism. By depositing lines of varying width, thickness, and spacing, as well as overlapping PE and PS lines, the authors elegantly demonstrated that the spatial sensitivity of this approach is more a consequence of tip sensitivity, and less limited by local heat transfer. Moreover, the authors were able to demonstrate the spectral sensitivity of this approach by resolving not only major backbone vibrational modes in the polymers themselves but also relatively weak scissor and ring modes. This raises the interesting question of correlating absorbance intensity as detected by the SPM cantilever with sample size

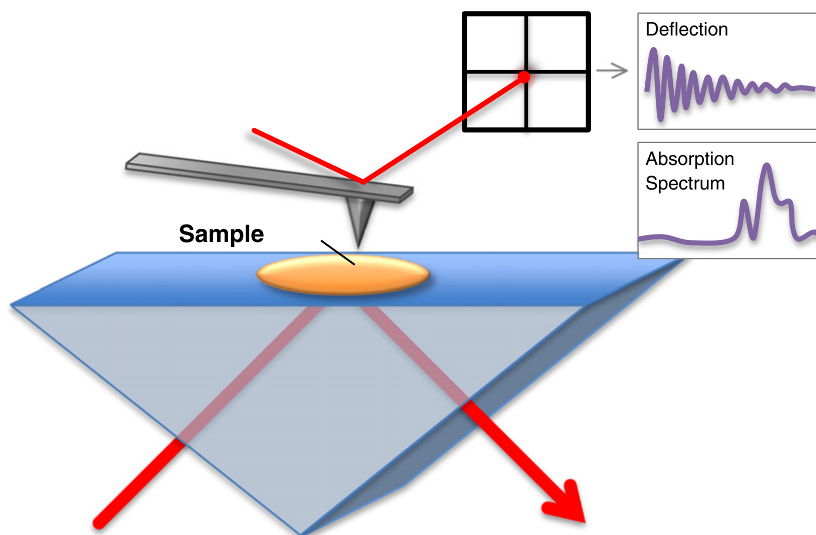


**Fig. 3.** Schematic representation of AFMIR/PTIR platform.

or more specifically thickness. While conventional FT-IR relies simply on differences in the relative absorbance as a function of wavelength, in the case of the PTIR approach, the detection and back-calculation to a relative absorbance measurement are coupled with a transfer function associated with photothermal conversion and thermomechanical expansion of the sample. What is the threshold sensitivity of the SPM cantilever to this thermomechanical effect and how does that correlate to the amount of material being sampled? What is the lower limit (i.e. minimum amount of sample that has to be present in order to generate a real signal)? This is particularly important when one is considering performing spatially super-resolved IR on individual molecular species. As has been clearly shown by Paulite et al., the tip-scattering based approach can readily resolve the spectra and structure of individual molecular fibrils (i.e. 5–8 nm thick fibrils) whereas in this PTIR work, the thinnest nanostructure was ~100 nm, a substantially thicker (and thus more strongly absorbing) feature [192]. Is there, for example, sufficient sensitivity (or response of the sample) for the PTIR approach to work on isolated individual ~5.5 nm thick membrane patches? This question certainly remains open and a tangible example of the critical challenges that remain.

During development of the PTIR platform, its relevance to the fields of materials and polymer science was quite clear. What was not as evident was its potential for biology and biophysical characterizations. In proof-of-concept work using the PTIR approach, Dazzi and others were able to acquire spatially resolved wavelength-dependent IR absorbance data on isolated bacteria [183,193–195]. While their initial work clearly demonstrated the ability of this approach to provide spatially resolved IR spectra, with strong absorbances at the Amide I and II bands present on the periphery of the bacteria, these data were convolved with tip geometry and field scattering effects within the sample itself. Moreover, while there was a clear correspondence between the IR data and the physical topography of the individual bacteria, there was no clear explanation as to why certain regions of the bacteria were devoid of Amide I and II absorption bands. It is not unreasonable to expect that the Amide I and II absorbances would be spatially ubiquitous in a biological sample and it is possible that some of these spatial variations may be artifactual. Given this consideration, scanning for more distinctive IR signatures would be more appropriate and this was the approach taken when the PTIR platform was used to examine bacteriophage-containing *Escherichia coli* [193]. Remarkably, in this work, the authors used the PTIR in a more quantitative fashion by focusing on regions of high IR absorbance, ~1050–1100 $cm^{-1}$ that are unique to DNA. Since bacteria lack a defined nucleus, their DNA is nominally homogeneously distributed throughout the cell body itself. This was nicely demonstrated in control images that clearly revealed a nominally uniform ~1050–1100 $cm^{-1}$ absorbance across the cell itself. When the cells were infected with phage, they were able to resolve a redistribution of the DNA-associated absorbances within the cell, and occasionally, isolated regions of higher intensity absorbance. These spatial differences were ascribed to the infection process itself, including cellular damage, and indeed the authors reported good correlations between the physical topography as mapped by the SPM, and spatial variations in absorbances. They also occasionally resolved localized absorbance intensities that they attributed to isolated phage particles. While these data are certainly illustrative of the ability of this platform to provide localized IR spectra using the SPM tip as effectively the detector, the spatial resolution remains somewhat suspect and indeed the authors were able to show computationally that the apparent physical width of the structures resolved spectroscopically is highly dependent on their location *within* the sample. In effect, the lateral resolution of the SPM-based spectral detection is now reflective of the local thermal characteristics. Since the SPM tip is arguably indirectly detecting the IR signature of the sample by measuring changes in the deflection response of the cantilever, heat dissipation within the sample itself will conspire to reduce the lateral resolution of this approach for examining structures buried within the sample.

Recently, Mayet et al., used this approach to examine a photosynthetic bacterium that naturally produces granules of polyhydroxybutyrate (PHB) [194]. In a remarkable series of experiments, the authors were able to demonstrate that the PTIR approach can spatially resolve sub-micron sized granules within bacteria and, more importantly, identify spectral differences that were attributed to different solid-state arrangements of PHB within the bacteria, as well as size effects. Indeed, the authors suggested that a ~7 $cm^{-1}$ shift in the characteristic ester C=O bond absorbance reflected the fact that PHB in the bacteria was in an amorphous rather than in crystalline form. This observation provides a compelling approach for investigating the physical and chemical changes that underpin the nucleation and growth of organized assemblies from their molecular constituents. In the context of cellular phenomena, it provides a particularly powerful strategy for examining bio-inspired crystallization and how living systems are able to template the formation of novel nanoscale structures and assemblies. Remarkably the authors were able to use the PTIR approach to now directly estimate the size of the nanogranules, finding that indeed they were similar in size to what they had previously seen by TEM. What was particularly intriguing about the PTIR strategy and which clearly illustrates the merits of a local, spatially resolved, measurement, was the authors' observation of a dramatic difference in the relative intensities of the PHB C=O band at ~1740 $cm^{-1}$ and the protein Amide I band at 1660 $cm^{-1}$ when measured by PTIR compared with conventional FTIR spectroscopy. Since the PTIR provides a more localized measurement, sampling over an isolated PHB granule in the bacterium itself yielded a much stronger PHB band compared to the protein Amide I band. This can be compared with conventional FT-IR spectroscopy wherein spectra are acquired over numerous bacteria and averaged. It is therefore not unreasonable to expect that at low PHB concentrations, it would become quite difficult to resolve the PHB C=O absorbance against a high background signal associated with the protein Amide I bond, which would reflect a low PHB to protein ratio in the bacteria (as a whole). Nevertheless, these results are clear evidence of the PTIR approach to provide sub-cellular chemical identification, and the ability to rapidly acquire spectra for structures that are well below the optical diffraction limit.

A clear advantage of IR spectroscopy over fluorescence is that it is a label-free approach, relying entirely on bond-specific energy absorption; however, this also presents a challenge in the sheer ubiquity of certain bonds (i.e. Amide I, Amide II), especially in biology. This raises the tantalizing possibility of introducing compounds that would have unique IR signatures and using the PTIR approach to map the location of these compounds within a cell or other biological structure. This was the approach recently reported by Policar et al., in which PTIR was used to track the distribution of a metal-carbonyl ligand in the cell [195]. Judicious selection of the metal-carbonyl bond allowed the authors to tune the PTIR system to a region of the IR spectrum that could be considered spectrally quiet. In this way, any spectral features that are seen clearly originate from the chosen ligand. In this case, the authors used a Re-tricarbonyl compound that has characteristic absorbances in the 2200–1800 $cm^{-1}$ range, well outside those associated with Amide I and II modes. By selecting specific regions of interest in the cell, and then scanning wavelengths of interest with the SPM tip on that location, PTIR nanoscopy can be performed and a full spectrum for that region can be generated. The authors presented a comprehensive strategy for localizing these metal-carbonyl ligands by selecting key IR absorbances and generating a "heat map" of these absorbances mapped against the physical shape and topography of the cell, as generated by the SPM simultaneously. Once "hot" spots were located, the SPM tip was placed on those specific regions and then a more detailed spectral scan acquired. Remarkably in this work, the authors were able to [1] map the location of the nucleus by scanning for regions of higher phosphate ($PO_2^-$) and amide absorbances; and [2] demonstrate

co-localization of the metal-carbonyl bond with these same regions. These data provided compelling evidence that the metal-carbonyl ligand was localized to the nucleus of the cell and portends the future use of this instrumentation platform in sub-cellular ligand imaging. Although one might argue that this is not really a truly label-free approach since one is necessarily adding a prosthetic group, this does raise the intriguing possibility of exploiting probes with unique IR signatures to track structures and interactions in live cells.

While these examples suggest that the PTIR approach has a number of key advantages, in the context of membrane proteins or protein–membrane interactions, a question remains as to whether there is sufficient absorption of IR energy in a single bilayer to afford a corresponding response in the SPM tip. It is also worth noting that much of the PTIR work has been done in air, rather than in fluid media. However, in a challenging proof of concept study, PTIR was applied successfully to afford IR spectra of individual living fungi in water [196]. In this work, the authors found that the response of the cantilever to the IR absorption differed substantially when immersed in water, reflecting largely the interactions with the surrounding media. Similar effects are well known for conventional SPM imaging in fluid media where changes in the mechanical response of the cantilever can be attributed to viscous damping effects. Since the PTIR approach relies on identifying and tracking the time-dependent response of the cantilever to the IR pulse, it is critical that the frequency response characteristics of the cantilever be clearly resolvable. While this is certainly the case when the cantilever is in air, once in liquid media, the amplitude of the frequency response can be damped significantly. Nevertheless, in this work, the authors found that the fundamental resonant frequency of the cantilever was a function of the surface that the cantilever was contacting with a shift of ~12 kHz for the cantilever immersed in water when it was in contact with the fungi versus the supporting ZnSe prism. This is particularly interesting since by simply tracking the cantilever response at either resonant frequency, it then becomes possible to clearly separate out IR absorbances due to the sample compared with bulk water. In this way, the authors were able to report a clearly resolvable IR absorbance at ~1080 $cm^{-1}$ for the glycogen absorption band for the cell wall. What is quite impressive about this approach is that by the IR sensitivity of the PTIR approach is directly tied to the cantilever's inherent mechanical response. If the SPM tip response is measured "off-resonance", scanning the IR spectrum and monitoring the tip response result in largely featureless spectral maps. It is only when one is measuring the "on-resonance" response that spectral contrast is achieved. The authors concluded by providing a compelling argument that there is no significant loss in either spectral sensitivity or topographical resolution when PTIR is performed in water.

A particularly compelling potential enhancement for the PTIR approach would be to exercise control over the polarization of the IR radiation. This would provide an exciting opportunity for determining molecular orientation and conformation, as has been applied in conventional polarization modulation-based techniques such as PM-IRRAS [92,197–199]. Such an implementation could be readily incorporated into the coupled ATR-IR/SPM geometry but would be more challenging in the context of the ANSIM platform.

## 5. Summary

The innovative integration of scanning probe microscopy with FT-IR spectroscopy has provided exciting new insights into the local structure, both chemical and topographical, of materials and biological samples. In this review, we have described three different approaches that have been used to date to provide this integration. The first focused on the physical mating of the two platform technologies. While this may be the simplest and most straightforward, affording full independent access to each platform's capabilities, it does not yet afford super-resolved IR spectra wherein the IR spectrum itself is co-localized to specific topographical features identified by the SPM. It does, however, provide much more ready access to the entire spectral range of interest, from near- through mid- to far-IR largely because of the low cost of the broadband IR sources and beamsplitters themselves. The ANSIM approach, which uses near field tip-based scattering, has shown tremendous potential for providing coupled super-resolved IR spectroscopy of individual protein fibrils, including tantalizing glimpses into local secondary structure. This approach certainly provides a strong complement to tip-enhanced Raman spectroscopy (TERS) [200,201]. It has tremendous potential for tracking protein– and peptide–membrane interactions including potentially identifying conformational changes upon membrane insertion. There remain however key challenges with the implementation of the ANSIM strategy, not the least of which relates to the appropriate selection of the IR light source. To date, only tunable IR lasers have been employed in ANSIM platforms and this necessarily limits the available spectral range. It is also unclear how well this platform will function in fluid media as to date, the applications of the tip-based scattering approaches (ANSIM, TERS) have been largely either in air or vacuum.

While still in its infancy, the PTIR hybrid approach to super-resolved IR spectra has generated considerable excitement in the community. With recent advances in tip design for increased sensitivity, its demonstrated ability to work in fluid media, and the potential of extrinsic probes with unique IR signatures, a wealth of opportunities exist for which this platform may prove ideal, including live cell mapping and characterization of extended surfaces. There are however key questions that remain including the sensitivity of the technique for true single molecule analysis, since the spectra are arguably generated indirectly through analysis of the cantilever's motion. The IR cross-section or absorption must be sufficiently large to yield a resolvable change in the cantilever's response. Whether this can be accommodated within a *single* molecule remains to be seen. As is the case with the ANSIM approach, the spectral range accessible to the system is limited by the characteristics of the laser itself and thus scanning a broad spectral range may require a complex laser combiner system. It is worth noting however that, as in the case of the coupled ATR-IR/SPM platform, the PTIR approach necessarily requires a supporting ATR crystal element, typically ZnSe. The surface roughness and chemistry of the crystal itself may adversely affect the structure and conformation of the adsorbed species. This may be a significant concern in the case of individual lipid bilayers or proteins adsorbed directly to the crystal surface. Indeed, for the PTIR studies of live cells, it was necessary to treat the ZnSe crystal appropriately to facilitate cell adhesion [196]. These considerations are less of an issue for the ANSIM approach since it requires an IR reflective substrate such as gold, which can be prepared as an atomically flat surface, ideal for SPM imaging, and readily modified with thiols and/or lipids as necessary.

This review has examined the potential that underpins the functional marriage of scanning probe microscopy with infrared spectroscopy. Arguably still in its infancy in terms of routine application in biophysics, it is clear that there is tremendous opportunity for novel insights that may be derived from the direct measurements of local molecular structure and topography that can be provided by these emerging platforms.

## References

[1] M. Bates, B. Huang, G.T. Dempsey, X. Zhuang, Multicolor super-resolution imaging with photo-switchable fluorescent probes, Science 317 (2007) 1749–1753.
[2] B. Huang, W. Wang, M. Bates, X. Zhuang, Three-dimensional super-resolution imaging by stochastic optical reconstruction microscopy, Science 319 (2008) 810–813.
[3] J. Lippincott-Schwartz, G.H. Patterson, Photoactivatable fluorescent proteins for diffraction-limited and super-resolution imaging, Trends Cell Biol. 19 (2009) 555–565.
[4] T.A. Brown, R.D. Fetter, A.N. Tkachuk, D.A. Clayton, Approaches toward super-resolution fluorescence imaging of mitochondrial proteins using palm, Methods 51 (2010) 458–463.
[5] B. Huang, Super-resolution optical microscopy: multiple choices, Curr. Opin. Chem. Biol. 14 (2010) 10–14.

[6] L. Schermelleh, R. Heintzmann, H. Leonhardt, A guide to super-resolution fluorescence microscopy, J. Cell Biol. 190 (2010) 165–175.
[7] B.O. Leung, K.C. Chou, Review of super-resolution fluorescence microscopy for biology, Appl. Spectrosc. 65 (2011) 967–980.
[8] S.A. Jones, S.H. Shim, J. He, X. Zhuang, Fast, three-dimensional super-resolution imaging of live cells, Nat. Methods 8 (2011) 499–508.
[9] S. Bakshi, B.P. Bratton, J.C. Weisshaar, Subdiffraction-limit study of kaede diffusion and spatial distribution in live escherichia coli, Biophys. J. 101 (2011) 2535–2544.
[10] S.M. Wiltgen, I.F. Smith, I. Parker, Superresolution localization of single functional ip3r channels utilizing $Ca^{2+}$ flux as a readout, Biophys. J. 99 (2010) 437–446.
[11] H. Park, E. Toprak, P.R. Selvin, Single-molecule fluorescence to study molecular motors, Q. Rev. Biophys. 40 (2007) 87–111.
[12] A. Yildiz, P.R. Selvin, Fluorescence imaging with one nanometer accuracy: application to molecular motors, Acc. Chem. Res. 38 (2005) 574–582.
[13] R. Zhang, E. Rothenberg, G. Fruhwirth, P.D. Simonson, F. Ye, I. Golding, T. Ng, W. Lopes, P.R. Selvin, Two-photon 3D FIONA of individual quantum dots in an aqueous environment, Nano Lett. 11 (2011) 4074–4078.
[14] T. Dertinger, R. Colyer, G. Iyer, S. Weiss, J. Enderlein, Fast, background-free, 3D super-resolution optical fluctuation imaging (SOFI), Proc. Natl. Acad. Sci. U. S. A. 106 (2009) 22287–22292.
[15] P. Dedecker, G.C. Mo, T. Dertinger, J. Zhang, Widely accessible method for superresolution fluorescence imaging of living systems, Proc. Natl. Acad. Sci. U. S. A. 109 (2012) 10909–10914.
[16] S. Geissbuehler, C. Dellagiacoma, T. Lasser, Comparison between SOFI and STORM, Biomed. Opt. Express 2 (2011) 408–420.
[17] T. Dertinger, R. Colyer, R. Vogel, J. Enderlein, S. Weiss, Achieving increased resolution and more pixels with superresolution optical fluctuation imaging (SOFI), Opt. Express 18 (2010) 18875–18885.
[18] T. Dertinger, R. Colyer, R. Vogel, M. Heilemann, M. Sauer, J. Enderlein, S. Weiss, Superresolution optical fluctuation imaging (SOFI), Adv. Exp. Med. Biol. 733 (2012) 17–21.
[19] J.E. Shaw, R.F. Epand, R.M. Epand, Z. Li, R. Bittman, C.M. Yip, Correlated fluorescence-atomic force microscopy of membrane domains: structure of fluorescence probes determines lipid localization, Biophys. J. 90 (2006) 2170–2178.
[20] J.R. Alattia, J.E. Shaw, C.M. Yip, G.G. Prive, Direct visualization of saposin remodelling of lipid bilayers, J. Mol. Biol. 362 (2006) 943–953.
[21] J.R. Alattia, J.E. Shaw, C.M. Yip, G.G. Prive, Molecular imaging of membrane interfaces reveals mode of beta-glucosidase activation by saposin c, Proc. Natl. Acad. Sci. U. S. A. 104 (2007) 17394–17399.
[22] J.E. Shaw, R.F. Epand, J.C. Hsu, G.C. Mo, R.M. Epand, C.M. Yip, Cationic peptide-induced remodelling of model membranes: direct visualization by in situ atomic force microscopy, J. Struct. Biol. 162 (2008) 121–138.
[23] J.E. Shaw, J.R. Alattia, J.E. Verity, G.G. Prive, C.M. Yip, Mechanisms of antimicrobial peptide action: studies of indolicidin assembly at model membrane interfaces by in situ atomic force microscopy, J. Struct. Biol. 154 (2006) 42–58.
[24] J.E. Shaw, A. Slade, C.M. Yip, Simultaneous in situ total internal reflectance fluorescence/atomic force microscopy studies of DPPC/dPOPC microdomains in supported planar lipid bilayers, J. Am. Chem. Soc. 125 (2003) 11838–11839.
[25] A.L. Slade, J.S. Schoeniger, D.Y. Sasaki, C.M. Yip, In situ scanning probe microscopy studies of tetanus toxin–membrane interactions, Biophys. J. 91 (2006) 4565–4574.
[26] A. Trache, S.M. Lim, Live cell response to mechanical stimulation studied by integrated optical and atomic force microscopy, J. Vis. Exp. 44 (2010) 2072.
[27] A. Trache, G.A. Meininger, Atomic force-multi-optical imaging integrated microscope for monitoring molecular dynamics in live cells, J. Biomed. Opt. 10 (2005) 064023.
[28] A. Trache, S.M. Lim, Integrated microscopy for real-time imaging of mechanotransduction studies in live cells, J. Biomed. Opt. 14 (2009) 034024.
[29] D.N. Fronczek, C. Quammen, H. Wang, C. Kisker, R. Superfine, R. Taylor, D.A. Erie, I. Tessmer, High accuracy FIONA-AFM hybrid imaging, Ultramicroscopy 111 (2011) 350–355.
[30] M.S. Kellermayer, Combined atomic force microscopy and fluorescence microscopy, Methods Mol. Biol. 736 (2011) 439–456.
[31] A.E. Brown, A. Hategan, D. Safer, Y.E. Goldman, D.E. Discher, Cross-correlated TIRF/AFM reveals asymmetric distribution of force-generating heads along self-assembled, “synthetic” myosin filaments, Biophys. J. 96 (2009) 1952–1960.
[32] R.J. Owen, C.D. Heyes, D. Knebel, C. Rocker, G.U. Nienhaus, An integrated instrumental setup for the combination of atomic force microscopy with optical spectroscopy, Biopolymers 82 (2006) 410–414.
[33] O. Coban, M. Burger, M. Laliberte, A. Ianoul, L.J. Johnston, Ganglioside partitioning and aggregation in phase-separated monolayers characterized by BODIBY GM1 monomer/dimer emission, Langmuir 23 (2007) 6704–6711.
[34] S. Zou Ira, D.M. Ramirez, S. Vanderlip, W. Ogilvie, Z.J. Jakubek, L.J. Johnston, Enzymatic generation of ceramide induces membrane restructuring: correlated AFM and fluorescence imaging of supported bilayers, J. Struct. Biol. 168 (2009) 78–89.
[35] Ira, L.J. Johnston, Sphingomyelinase generation of ceramide promotes clustering of nanoscale domains in supported bilayer membranes, Biochim. Biophys. Acta 1778 (2008) 185–197.
[36] K. Ono, M.M. Condron, D.B. Teplow, Structure-neurotoxicity relationships of amyloid beta-protein oligomers, Proc. Natl. Acad. Sci. U. S. A. 106 (2009) 14745–14750.
[37] S. Grudzielanek, A. Velkova, A. Shukla, V. Smirnovas, M. Tatarek-Nossol, H. Rehage, A. Kapurniotu, R. Winter, Cytotoxicity of insulin within its self-assembly and amyloidogenic pathways, J. Mol. Biol. 370 (2007) 372–384.
[38] N. Sarkar, M. Kumar, V.K. Dubey, Rottlerin dissolves pre-formed protein amyloid: a study on hen egg white lysozyme, Biochim. Biophys. Acta 1810 (2011) 809–814.
[39] H. Jang, F.T. Arce, M. Mustata, S. Ramachandran, R. Capone, R. Nussinov, R. Lal, Antimicrobial protegrin-1 forms amyloid-like fibrils with rapid kinetics suggesting a functional link, Biophys. J. 100 (2011) 1775–1783.
[40] T. Fukuma, A.S. Mostaert, L.C. Serpell, S.P. Jarvis, Revealing molecular-level surface structure of amyloid fibrils in liquid by means of frequency modulation atomic force microscopy, Nanotechnology 19 (2008) 384010.
[41] M.C. Manning, Use of infrared spectroscopy to monitor protein structure and stability, Expert Rev. Proteomics 2 (2005) 731–743.
[42] H. Hiramatsu, T. Kitagawa, FT-IR approaches on amyloid fibril structure, Biochim. Biophys. Acta 1753 (2005) 100–107.
[43] H. Fabian, D. Naumann, Methods to study protein folding by stopped-flow FT-IR, Methods 34 (2004) 28–40.
[44] Z. Ganim, H.S. Chung, A.W. Smith, L.P. Deflores, K.C. Jones, A. Tokmakoff, Amide I two-dimensional infrared spectroscopy of proteins, Acc. Chem. Res. 41 (2008) 432–441.
[45] C. Kotting, K. Gerwert, Proteins in action monitored by time-resolved FTIR spectroscopy, Chemphyschem 6 (2005) 881–888.
[46] J.T. Kennis, M.L. Groot, Ultrafast spectroscopy of biological photoreceptors, Curr. Opin. Struct. Biol. 17 (2007) 623–630.
[47] T. Noguchi, Light-induced ftir difference spectroscopy as a powerful tool toward understanding the molecular mechanism of photosynthetic oxygen evolution, Photosynth. Res. 91 (2007) 59–69.
[48] C. Jung, Fourier transform infrared spectroscopy as a tool to study structural properties of cytochromes p450 (CYPS), Anal. Bioanal. Chem. 392 (2008) 1031–1058.
[49] P. Hamm, J. Helbing, J. Bredenbeck, Two-dimensional infrared spectroscopy of photoswitchable peptides, Annu. Rev. Phys. Chem. 59 (2008) 291–317.
[50] N.T. Hunt, 2d-IR spectroscopy: ultrafast insights into biomolecule structure and function, Chem. Soc. Rev. 38 (2009) 1837–1848.
[51] A. Lewandowska, S. Oldziej, A. Liwo, H.A. Scheraga, Beta-hairpin-forming peptides; models of early stages of protein folding, Biophys. Chem. 151 (2010) 1–9.
[52] M. Carbonaro, A. Nucara, Secondary structure of food proteins by Fourier Transform spectroscopy in the mid-infrared region, Amino Acids 38 (2010) 679–690.
[53] E. Goormaghtigh, V. Raussens, J.M. Ruysschaert, Attenuated total reflection infrared spectroscopy of proteins and lipids in biological membranes, Biochim. Biophys. Acta 1422 (1999) 105–185.
[54] L.K. Tamm, S.A. Tatulian, Infrared spectroscopy of proteins and peptides in lipid bilayers, Q. Rev. Biophys. 30 (1997) 365–429.
[55] H.U. Gremlich, U.P. Fringeli, R. Schwyzer, Conformational changes of adrenocorticotropin peptides upon interaction with lipid membranes revealed by infrared attenuated total reflection spectroscopy, Biochemistry 22 (1983) 4257–4264.
[56] H.U. Gremlich, U.P. Fringeli, R. Schwyzer, Interaction of adrenocorticotropin-(11-24)-tetradecapeptide with neutral lipid membranes revealed by infrared attenuated total reflection spectroscopy, Biochemistry 23 (1984) 1808–1810.
[57] D. Erne, R. Schwyzer, Membrane structure of bombesin studied by infrared spectroscopy. Prediction of membrane interactions of gastrin-releasing peptide, neuromedin B, and neuromedin C, Biochemistry 26 (1987) 6316–6319.
[58] H.H. Bauer, M. Muller, J. Goette, H.P. Merkle, U.P. Fringeli, Interfacial adsorption and aggregation associated changes in secondary structure of human calcitonin monitored by ATR-FTIR spectroscopy, Biochemistry 33 (1994) 12276–12282.
[59] S. Badilescu, C. Sandorfy, Infrared attenuated total reflection spectroscopic studies on the hydration of the Gramicidin A transmembrane channel, J. Mol. Struct. 189 (1988) 31–42.
[60] Z. Kota, T. Pali, D. Marsh, Orientation and lipid-peptide interactions of gramicidin a in lipid membranes: polarized attenuated total reflection infrared spectroscopy and spin-label electron spin resonance, Biophys. J. 86 (2004) 1521–1531.
[61] E. Okamura, J. Umemura, T. Takenaka, Orientation of gramicidin d incorporated into phospholipid multibilayers: a Fourier Transform infrared-attenuated total reflection spectroscopic study, Biochim. Biophys. Acta Biomembr. 856 (1986) 68–75.
[62] A. Ausili, S. Corbalan-Garcia, J.C. Gomez-Fernandez, D. Marsh, Membrane docking of the c2 domain from protein kinase calpha as seen by polarized ATR-IR. The role of PIP(2), Biochim. Biophys. Acta 1808 (2011) 684–695.
[63] J. Thundimadathil, R.W. Roeske, L. Guo, A synthetic peptide forms voltage-gated porin-like ion channels in lipid bilayer membranes, Biochem. Biophys. Res. Commun. 330 (2005) 585–590.
[64] J. Thundimadathil, R.W. Roeske, L. Guo, Effect of membrane mimicking environment on the conformation of a pore-forming (XSXG)6 peptide, Biopolymers 84 (2006) 317–328.
[65] S. Castano, B. Desbat, Structure and orientation study of fusion peptide fp23 of gp41 from hiv-1 alone or inserted into various lipid membrane models (mono-, bi- and multibi-layers) by FT-IR spectroscopies and Brewster angle microscopy, Biochim. Biophys. Acta Biomembr. 1715 (2005) 81–95.
[66] I. Martin, H. Schaal, A. Scheid, J.M. Ruysschaert, Lipid membrane fusion induced by the human immunodeficiency virus type 1 GP41 n-terminal extremity is determined by its orientation in the lipid bilayer, J. Virol. 70 (1996) 298–304.
[67] I.T. Arkin, M. Rothman, C.F.C. Ludlam, S. Aimoto, D.M. Engelman, K.J. Rothschild, S.O. Smith, Structural model of the phospholamban ion channel complex in phospholipid membranes, J. Mol. Biol. 248 (1995) 824–834.
[68] A. Le Saux, J.M. Ruysschaert, E. Goormaghtigh, Membrane molecule reorientation in an electric field recorded by attenuated total reflection Fourier-transform infrared spectroscopy, Biophys. J. 80 (2001) 324–330.
[69] J. Corbin, N. Methot, H.H. Wang, J.E. Baenziger, M.P. Blanton, Secondary structure analysis of individual transmembrane segments of the nicotinic acetylcholine receptor by circular dichroism and Fourier transform infrared spectroscopy, J. Biol. Chem. 273 (1998) 771–777.
[70] S.E. Ryan, H.P. Nguyen, J.E. Baenziger, Anesthetic-induced structural changes in the nicotinic acetylcholine receptor, Toxicol. Lett. 100–101 (1998) 179–183.

[71] J.S. Sharp, J.A. Forrest, R.A. Jones, Surface denaturation and amyloid fibril formation of insulin at model lipid–water interfaces, Biochemistry 41 (2002) 15810–15819.
[72] P. Cai, C.R. Flach, R. Mendelsohn, An infrared reflection–absorption spectroscopy study of the secondary structure in (KL4)4K, a therapeutic agent for respiratory distress syndrome, in aqueous monolayers with phospholipids, Biochemistry 42 (2003) 9446–9452.
[73] M. Kasbauer, T.M. Bayerl, Formation of domains of cationic or anionic lipids in binary lipid mixtures increases the electrostatic coupling strength of water-soluble proteins to supported bilayers, Biochemistry 38 (1999) 15258–15263.
[74] M. Kasbauer, M. Junglas, T.M. Bayerl, Effect of cationic lipids in the formation of asymmetries in supported bilayers, Biophys. J. 76 (1999) 2600–2605.
[75] S. Terrettaz, W.P. Ulrich, H. Vogel, Q. Hong, L.G. Dover, J.H. Lakey, Stable self-assembly of a protein engineering scaffold on gold surfaces, Protein Sci. 11 (2002) 1917–1925.
[76] D. Avrahami, Y. Shai, A new group of antifungal and antibacterial lipopeptides derived from non-membrane active peptides conjugated to palmitic acid, J. Biol. Chem. 279 (2004) 12277–12285.
[77] K. Sackett, Y. Shai, The HIV fusion peptide adopts intermolecular parallel beta-sheet structure in membranes when stabilized by the adjacent n-terminal heptad repeat: a 13C FTIR study, J. Mol. Biol. 350 (2005) 790–805.
[78] A. Lorin, B. Charloteaux, Y. Fridmann-Sirkis, A. Thomas, Y. Shai, R. Brasseur, Mode of membrane interaction and fusogenic properties of a de novo transmembrane model peptide depend on the length of the hydrophobic core, J. Biol. Chem. 282 (2007) 18388–18396.
[79] A.M. Alaouie, R.N. Lewis, R.N. McElhaney, Differential scanning calorimetry and Fourier transform infrared spectroscopic studies of phospholipid organization and lipid–peptide interactions in nanoporous substrate-supported lipid model membranes, Langmuir 23 (2007) 7229–7234.
[80] R.N. Lewis, M. Kiricsi, E.J. Prenner, R.S. Hodges, R.N. McElhaney, Fourier transform infrared spectroscopic study of the interactions of a strongly antimicrobial but weakly hemolytic analogue of Gramicidin S with lipid micelles and lipid bilayer membranes, Biochemistry 42 (2003) 440–449.
[81] G.W. Seto, S. Marwaha, D.M. Kobewka, R.N. Lewis, F. Separovic, R.N. McElhaney, Interactions of the Australian tree frog antimicrobial peptides aurein 1.2, citropin 1.1 and maculatin 1.1 with lipid model membranes: differential scanning calorimetric and Fourier transform infrared spectroscopic studies, Biochim. Biophys. Acta 1768 (2007) 2787–2800.
[82] J. Seeliger, K. Weise, N. Opitz, R. Winter, The effect of ABeta on IAPP aggregation in the presence of an isolated beta-cell membrane, J. Mol. Biol. 421 (2012) 348–363.
[83] P. Rigler, W.P. Ulrich, R. Hovius, E. Ilegems, H. Pick, H. Vogel, Downscaling Fourier transform infrared spectroscopy to the micrometer and nanogram scale: secondary structure of serotonin and acetylcholine receptors, Biochemistry 42 (2003) 14017–14022.
[84] R. Mendelsohn, G. Mao, C.R. Flach, Infrared reflection–absorption spectroscopy: principles and applications to lipid–protein interaction in langmuir films, Biochim. Biophys. Acta 1798 (2010) 788–800.
[85] Z. Xu, J.W. Brauner, C.R. Flach, R. Mendelsohn, Orientation of peptides in aqueous monolayer films. Infrared reflection–absorption spectroscopy studies of a synthetic amphipathic beta-sheet, Langmuir 20 (2004) 3730–3733.
[86] M. Nullmeier, H. Koliwer-Brandl, S. Kelm, P. Zagel, K.W. Koch, I. Brand, Impact of strong and weak lipid–protein interactions on the structure of a lipid bilayer on a gold electrode surface, Chemphyschem 12 (2011) 1066–1079.
[87] L. Wang, J.W. Brauner, G. Mao, E. Crouch, B. Seaton, J. Head, K. Smith, C.R. Flach, R. Mendelsohn, Interaction of recombinant surfactant protein D with lipopolysaccharide: conformation and orientation of bound protein by IRRAS and simulations, Biochemistry 47 (2008) 8103–8113.
[88] F. Ronzon, B. Desbat, J.P. Chauvet, B. Roux, Behavior of a GPI-anchored protein in phospholipid monolayers at the air–water interface, Biochim. Biophys. Acta 1560 (2002) 1–13.
[89] D. Dieudonne, R. Mendelsohn, R.S. Farid, C.R. Flach, Secondary structure in lung surfactant SP-B peptides: IR and CD studies of bulk and monolayer phases, Biochim. Biophys. Acta 1511 (2001) 99–112.
[90] X. Bin, S.L. Horswell, J. Lipkowski, Electrochemical and PM-IRRAS studies of the effect of cholesterol on the structure of a DMPC bilayer supported at an Au (111) electrode surface, part 1: properties of the acyl chains, Biophys. J. 89 (2005) 592–604.
[91] X. Bin, I. Zawisza, J.D. Goddard, J. Lipkowski, Electrochemical and PM-IRRAS studies of the effect of the static electric field on the structure of the DMPC bilayer supported at a Au(111) electrode surface, Langmuir 21 (2005) 330–347.
[92] N. Garcia-Araez, C.L. Brosseau, P. Rodriguez, J. Lipkowski, Layer-by-layer PMIRRAS characterization of DMPC bilayers deposited on a Au111 electrode surface, Langmuir 22 (2006) 10365–10371.
[93] Y. Itoh, M. Muro, T. Hasegawa, Quality evaluation of polarization-modulation infrared reflection–absorption spectra of a langmuir monolayer on water dependent on angle of incidence and molecular orientation, Appl. Spectrosc. 64 (2010) 1374–1378.
[94] R.D. Herculano, F.J. Pavinatto, L. Caseli, C. D'Silva, O.N. Oliveira Jr., The lipid composition of a cell membrane modulates the interaction of an antiparasitic peptide at the air–water interface, Biochim. Biophys. Acta 1808 (2011) 1907–1912.
[95] G. Matar, F. Besson, Influence of the lipid composition of biomimetic monolayers on the structure and orientation of the GP41 tryptophan-rich peptide from HIV-1, Biochim. Biophys. Acta 1808 (2011) 2534–2543.
[96] V.A. Lorenz-Fonfria, M. Granell, X. Leon, G. Leblanc, E. Padros, In-plane and out-of-plane infrared difference spectroscopy unravels tilting of helices and structural changes in a membrane protein upon substrate binding, J. Am. Chem. Soc. 131 (2009) 15094–15095.
[97] G. Zhang, D.J. Moore, C.R. Flach, R. Mendelsohn, Vibrational microscopy and imaging of skin: from single cells to intact tissue, Anal. Bioanal. Chem. 387 (2007) 1591–1599.
[98] G. Zhang, D.J. Moore, R. Mendelsohn, C.R. Flach, Vibrational microspectroscopy and imaging of molecular composition and structure during human corneocyte maturation, J. Invest. Dermatol. 126 (2006) 1088–1094.
[99] H. Ouyang, P.J. Sherman, E.P. Paschalis, A.L. Boskey, R. Mendelsohn, Fourier transform infrared microscopic imaging: effects of estrogen and estrogen deficiency on fracture healing in rat femurs, Appl. Spectrosc. 58 (2004) 1–9.
[100] G. Mao, C.R. Flach, R. Mendelsohn, R.M. Walters, Imaging the distribution of sodium dodecyl sulfate in skin by confocal Raman and infrared microspectroscopy, Pharm. Res. 29 (2012) 2189–2201.
[101] S. Gourion-Arsiquaud, J.C. Burket, L.M. Havill, E. DiCarlo, S.B. Doty, R. Mendelsohn, M.C. van der Meulen, A.L. Boskey, Spatial variation in osteonal bone properties relative to tissue and animal age, J. Bone Miner. Res. 24 (2009) 1271–1281.
[102] R. Mendelsohn, A. Hassankhani, E. DiCarlo, A. Boskey, Ft-ir microscopy of endochondral ossification at 20 mu spatial resolution, Calcif. Tissue Int. 44 (1989) 20–24.
[103] R. Noreen, M. Moenner, Y. Hwu, C. Petibois, FTIR spectro-imaging of collagens for characterization and grading of gliomas, Biotechnol. Adv. 30 (2012) 1432–1446.
[104] L. Quaroni, T. Zlateva, Infrared spectromicroscopy of biochemistry in functional single cells, Analyst 136 (2011) 3219–3232.
[105] C.H. Petter, N. Heigl, M. Rainer, R. Bakry, J. Pallua, G.K. Bonn, C.W. Huck, Development and application of Fourier-transform infrared chemical imaging of tumour in human tissue, Curr. Med. Chem. 16 (2009) 318–326.
[106] X. Wang, Z. Qi, S. Wang, G. Liu, H. Gao, Y. Tian, The study of a single BGC823 cell using Fourier transform infrared microspectroscopic imaging, Spectrochim. Acta A Mol. Biomol. Spectrosc. 79 (2011) 1660–1662.
[107] H.A. Bechtel, M.C. Martin, T.E. May, P. Lerch, Improved spatial resolution for reflection mode infrared microscopy, Rev. Sci. Instrum. 80 (2009) 126106.
[108] C. Petibois, M. Cestelli-Guidi, M. Piccinini, M. Moenner, A. Marcelli, Synchrotron radiation FTIR imaging in minutes: a first step towards real-time cell imaging, Anal. Bioanal. Chem. 397 (2010) 2123–2129.
[109] P. Bassan, A. Sachdeva, A. Kohler, C. Hughes, A. Henderson, J. Boyle, J.H. Shanks, M. Brown, N.W. Clarke, P. Gardner, FTIR microscopy of biological cells and tissue: data analysis using resonant Mie scattering (RMIES) emsc algorithm, Analyst 137 (2012) 1370–1377.
[110] P. Garidel, M. Boese, Mid infrared microspectroscopic mapping and imaging: a bio-analytical tool for spatially and chemically resolved tissue characterization and evaluation of drug permeation within tissues, Microsc. Res. Tech. 70 (2007) 336–349.
[111] A. Gorzsas, H. Stenlund, P. Persson, J. Trygg, B. Sundberg, Cell-specific chemotyping and multivariate imaging by combined FT-IR microspectroscopy and orthogonal projections to latent structures (OPLS) analysis reveals the chemical landscape of secondary xylem, Plant J. 66 (2011) 903–914.
[112] M. Isenor, S.G. Kaminskyj, R.J. Rodriguez, R.S. Redman, K.M. Gough, Characterization of mannitol in curvularia protuberata hyphae by FTIR and Raman spectromicroscopy, Analyst 135 (2010) 3249–3254.
[113] M.A. Poggi, E.D. Gadsby, L.A. Bottomley, W.P. King, E. Oroudjev, H. Hansma, Scanning probe microscopy, Anal. Chem. 76 (2004) 3429–3443.
[114] R.G. Creasey, C.T. Gibson, N.H. Voelcker, Characterization of fiber-forming peptides and proteins by means of atomic force microscopy, Curr. Protein Pept. Sci. 13 (2012) 232–257.
[115] T. Ando, High-speed atomic force microscopy coming of age, Nanotechnology 23 (2012) 062001.
[116] I. Casuso, F. Rico, S. Scheuring, Biological AFM: where we come from–where we are–where we may go, J. Mol. Recognit. 24 (2011) 406–413.
[117] P.L. Frederix, P.D. Bosshart, A. Engel, Atomic force microscopy of biological membranes, Biophys. J. 96 (2009) 329–338.
[118] K. El Kirat, S. Morandat, Y.F. Dufrene, Nanoscale analysis of supported lipid bilayers using atomic force microscopy, Biochim. Biophys. Acta 1798 (2010) 750–765.
[119] S. Amemiya, J. Guo, H. Xiong, D.A. Gross, Biological applications of scanning electrochemical microscopy: chemical imaging of single living cells and beyond, Anal. Bioanal. Chem. 386 (2006) 458–471.
[120] D.P. Allison, N.P. Mortensen, C.J. Sullivan, M.J. Doktycz, Atomic force microscopy of biological samples, Wiley Interdiscip. Rev. Nanomed. Nanobiotechnol. 2 (2010) 618–634.
[121] S. Moreno Flores, J.L. Toca-Herrera, The new future of scanning probe microscopy: combining atomic force microscopy with other surface-sensitive techniques, optical microscopy and fluorescence techniques, Nanoscale 1 (2009) 40–49.
[122] M. Brucherseifer, C. Kranz, B. Mizaikoff, Combined in situ atomic force microscopy-infrared-attenuated total reflection spectroscopy, Anal. Chem. 79 (2007) 8803–8806.
[123] J.E. Verity, N. Chhabra, K. Sinnathamby, C.M. Yip, Tracking molecular interactions in membranes by simultaneous ATR-FTIR–SPM, Biophys. J. 97 (2009) 1225–1231.
[124] B. Knoll, F. Keilmann, Mid-infrared scanning near-field optical microscope resolves 30 nm, J. Microsc. 194 (1999) 512–515.
[125] G. Yang, K.A. Woodhouse, C.M. Yip, Substrate-facilitated assembly of elastin-like peptides: studies by variable-temperature in situ atomic force microscopy, J. Am. Chem. Soc. 124 (2002) 10648–10649.
[126] M.C. Hull, L.R. Cambrea, J.S. Hovis, Infrared spectroscopy of fluid lipid bilayers, Anal. Chem. 77 (2005) 6096–6099.
[127] R. Hillenbrand, T. Taubner, F. Keilmann, Phonon-enhanced light-matter interaction at the nanometre scale, Nature 418 (2002) 159–162.
[128] F. Keilmann, Vibrational-infrared near-field microscopy, Vib. Spectrosc. 29 (2002) 109–114.

[129] A. Lahrech, R. Bachelot, P. Gleyzes, A.C. Boccara, Infrared near-field imaging of implanted semiconductors: evidence of a pure dielectric contrast, Appl. Phys. Lett. 71 (1997) 575–577.
[130] R. Bachelot, P. Gleyzes, A.C. Boccara, Reflection-mode scanning near-field optical microscopy using an apertureless metallic tip, Appl. Opt. 36 (1997) 2160–2170.
[131] A. Lahrech, R. Bachelot, P. Gleyzes, A.C. Boccara, Infrared-reflection-mode near-field microscopy using an apertureless probe with a resolution of lambda/600, Opt. Lett. 21 (1996) 1315–1317.
[132] B. Knoll, F. Keilmann, Scanning microscopy by mid-infrared near-field scattering, Appl. Phys. A-Mater. 66 (1998) 477–481.
[133] B. Knoll, F. Keilmann, Mid-infrared scanning near-field optical microscope resolves 30 nm, J. Microsc. (Oxf.) 194 (1999) 512–515.
[134] F. Keilmann, B. Knoll, A. Kramer, Long-wave-infrared near-field microscopy, Phys. Status Solidi B 215 (1999) 849–854.
[135] B. Knoll, F. Keilmann, Near-field probing of vibrational absorption for chemical microscopy, Nature 399 (1999) 134–137.
[136] K. Mueller, X. Yang, M. Paulite, Z. Fakhraai, N. Gunari, G.C. Walker, Chemical imaging of the surface of self-assembled polystyrene-b-poly(methyl methacrylate) diblock copolymer films using apertureless near-field IR microscopy, Langmuir 24 (2008) 6946–6951.
[137] B.B. Akhremitchev, G.C. Walker, Developing vibrational infrared near field spectroscopy to characterize polymer structures on surfaces: identification and reduction of topographic coupling artifacts, Bull. Chem. Soc. Jpn. 75 (2002) 1011–1018.
[138] B.B. Akhremitchev, S. Pollack, G.C. Walker, Apertureless scanning near-field infrared microscopy of a rough polymeric surface, Langmuir 17 (2001) 2774–2781.
[139] B.B. Akhremitchev, G.C. Walker, Apertureless near-field scanning ir microscopy of rough surfaces, Abstr. Pap. Am. Chem. Soc. 221 (2001) U71.
[140] H.J. Li, D. Wei, S.N. Piramanayagam, Micromagnetic studies on resolution limits of magnetic force microscopy tips with different magnetic anisotropy, J. Appl. Phys. 111 (2012).
[141] B.I. Kim, Effects of long-range tip-sample interaction on magnetic force imaging: a comparative study between bimorph driven system and electrostatic force modulation, J. Appl. Phys. 111 (2012).
[142] K. Liu, S.B. Clendenning, L. Friebe, W.Y. Chan, X.B. Zhu, M.R. Freeman, G.C. Yang, C.M. Yip, D. Grozea, Z.H. Lu, I. Manners, Pyrolysis of highly metallized polymers: ceramic thin films containing magnetic cofe alloy nanoparticles from a polyferrocenylsilane with pendant cobalt clusters, Chem. Mater. 18 (2006) 2591–2601.
[143] V. Romanov, G.C. Walker, Infrared near-field detection of a narrow resonance due to molecular vibrations in a nanoparticle, Langmuir 23 (2007) 2829–2837.
[144] M. Paulite, Z. Fakhraai, I.T.S. Li, N. Gunari, A.E. Tanur, G.C. Walker, Nanoscale imaging of the secondary structure of individual amyloid fibrils made from a beta(2)-microglobulin fragment using near-field infrared microscopy, Abstr. Pap. Am. Chem. Soc. 242 (2011).
[145] C.M. Yip, J. McLaurin, Amyloid-beta peptide assembly: a critical step in fibrillogenesis and membrane disruption, Biophys. J. 80 (2001) 1359–1371.
[146] C.M. Yip, E.A. Elton, A.A. Darabie, M.R. Morrison, J. McLaurin, Cholesterol, a modulator of membrane-associated Abeta-fibrillogenesis and neurotoxicity, J. Mol. Biol. 311 (2001) 723–734.
[147] J. Yau, S. Sharpe, Structures of amyloid fibrils formed by the prion protein derived peptides prp(244–249) and prp(245–250), J. Struct. Biol. 180 (2012) 290–302.
[148] P. Walsh, J. Yau, K. Simonetti, S. Sharpe, Morphology and secondary structure of stable beta-oligomers formed by amyloid peptide PrP(106–126), Biochemistry 48 (2009) 5779–5781.
[149] R.S. Harrison, P.C. Sharpe, Y. Singh, D.P. Fairlie, Amyloid peptides and proteins in review, Rev. Physiol. Biochem. Pharmacol. 159 (2007) 1–77.
[150] C.T. Middleton, P. Marek, P. Cao, C.C. Chiu, S. Singh, A.M. Woys, J.J. de Pablo, D.P. Raleigh, M.T. Zanni, Two-dimensional infrared spectroscopy reveals the complex behaviour of an amyloid fibril inhibitor, Nat. Chem. 4 (2012) 355–360.
[151] Y. Guo, J. Wang, Spectroscopic evidence for polymorphic aggregates formed by amyloid-beta fragments, Chemphyschem 13 (2012) 3901–3908.
[152] S. Fukunaga, H. Ueno, T. Yamaguchi, Y. Yano, M. Hoshino, K. Matsuzaki, Gm1 cluster mediates formation of toxic Abeta fibrils by providing hydrophobic environments, Biochemistry 51 (41) (2012) 8125–8131.
[153] J.C. Rodriguez-Perez, I.W. Hamley, A.M. Squires, Infrared linear dichroism spectroscopy on amyloid fibrils aligned by molecular combing, Biomacromolecules 12 (2011) 1810–1821.
[154] Y.L. Ling, D.B. Strasfeld, S.H. Shim, D.P. Raleigh, M.T. Zanni, Two-dimensional infrared spectroscopy provides evidence of an intermediate in the membrane-catalyzed assembly of diabetic amyloid, J. Phys. Chem. B 113 (2009) 2498–2505.
[155] J. Juarez, P. Taboada, V. Mosquera, Existence of different structural intermediates on the fibrillation pathway of human serum albumin, Biophys. J. 96 (2009) 2353–2370.
[156] N. Cerda-Costa, I. De la Arada, F.X. Aviles, J.L. Arrondo, S. Villegas, Influence of aggregation propensity and stability on amyloid fibril formation as studied by Fourier transform infrared spectroscopy and two-dimensional cos analysis, Biochemistry 48 (2009) 10582–10590.
[157] A. Peralvarez-Marin, A. Barth, A. Graslund, Time-resolved infrared spectroscopy of pH-induced aggregation of the Alzheimer Abeta(1–28) peptide, J. Mol. Biol. 379 (2008) 589–596.
[158] T.R. Jahn, G.A. Tennent, S.E. Radford, A common beta-sheet architecture underlies in vitro and in vivo beta2-microglobulin amyloid fibrils, J. Biol. Chem. 283 (2008) 17279–17286.
[159] L.L. del Mercato, G. Maruccio, P.P. Pompa, B. Bochicchio, A.M. Tamburro, R. Cingolani, R. Rinaldi, Amyloid-like fibrils in elastin-related polypeptides: structural characterization and elastic properties, Biomacromolecules 9 (2008) 796–803.
[160] O.S. Makin, L.C. Serpell, Examining the structure of the mature amyloid fibril, Biochem. Soc. Trans. 30 (2002) 521–525.
[161] A. Parbhu, H. Lin, J. Thimm, R. Lal, Imaging real-time aggregation of amyloid beta protein (1–42) by atomic force microscopy, Peptides 23 (2002) 1265–1270.
[162] W.S. Gosal, S.L. Myers, S.E. Radford, N.H. Thomson, Amyloid under the atomic force microscope, Protein Pept. Lett. 13 (2006) 261–270.
[163] P. Marek, A. Abedini, B. Song, M. Kanungo, M.E. Johnson, R. Gupta, W. Zaman, S.S. Wong, D.P. Raleigh, Aromatic interactions are not required for amyloid fibril formation by islet amyloid polypeptide but do influence the rate of fibril formation and fibril morphology, Biochemistry 46 (2007) 3255–3261.
[164] W.J. Cho, B.P. Jena, A.M. Jeremic, Nano-scale imaging and dynamics of amylin–membrane interactions and its implication in type ii diabetes mellitus, Methods Cell Biol. 90 (2008) 267–286.
[165] F.T. Arce, H. Jang, S. Ramachandran, P.B. Landon, R. Nussinov, R. Lal, Polymorphism of amyloid beta peptide in different environments: implications for membrane insertion and pore formation, Soft Matter 7 (2011) 5267–5273.
[166] H. LeVine III, Stopped-flow kinetics reveal multiple phases of thioflavin t binding to Alzheimer beta (1–40) amyloid fibrils, Arch. Biochem. Biophys. 342 (1997) 306–316.
[167] F. Chiti, P. Mangione, A. Andreola, S. Giorgetti, M. Stefani, C.M. Dobson, V. Bellotti, N. Taddei, Detection of two partially structured species in the folding process of the amyloidogenic protein beta 2-microglobulin, J. Mol. Biol. 307 (2001) 379–391.
[168] X. Du, T. Zhang, R. Li, K. Wang, Nature of cerium(III)- and lanthanum(III)-induced aggregation of human erythrocyte membrane proteins, J. Inorg. Biochem. 84 (2001) 67–75.
[169] Q. Xu, T.A. Keiderling, Trifluoroethanol-induced unfolding of Concanavalin A: equilibrium and time-resolved optical spectroscopic studies, Biochemistry 44 (2005) 7976–7987.
[170] F. Huth, A. Govyadinov, S. Amarie, W. Nuansing, F. Keilmann, R. Hillenbrand, Nano-FTIR absorption spectroscopy of molecular fingerprints at 20 nm spatial resolution, Nano Lett. 12 (2012) 3973–3978.
[171] D.T. Schaafsma, R. Mossadegh, J.S. Sanghera, I.D. Aggarwal, M. Luce, R. Generosi, P. Perfetti, A. Cricenti, J.M. Gilligan, N.H. Tolk, Fabrication of single-mode chalcogenide fiber probes for scanning near-field infrared optical microscopy, Opt. Eng. 38 (1999) 1381–1385.
[172] A. Cricenti, G. Longo, V. Mussi, R. Generosi, M. Luce, P. Perfetti, A. Vobornik, G. Margaritondo, P. Thielen, J.S. Sanghera, I.D. Aggarwal, N.H. Tolk, G. Baldacchini, F. Bonfigli, F. Flora, T. Marolo, R.M. Montereali, A. Faenov, T. Pikuz, F. Somma, D.W. Piston, Ir-snom on lithium fluoride films with regular arrays based on colour centres, Phys. Status Solidi C (2003) 3075–3080, (Vol 0, No 8 0).
[173] D. Vobornik, G. Margaritondo, J.S. Sanghera, P. Thielen, I.D. Aggarwal, B. Ivanov, N.H. Tolk, V. Manni, S. Grimaldi, A. Lisi, S. Rieti, D.W. Piston, R. Generosi, M. Luce, P. Perfetti, A. Cricenti, Spectroscopic infrared scanning near-field optical microscopy (IR-SNOM), J. Alloys Compd. 401 (2005) 80–85.
[174] D. Vobornik, G. Margaritondo, S. Vobornik, P. Thielen, R. Generosi, N. Tolk, A. Cricenti, Very high resolution chemical imaging with infrared scanning near-field optical microscopy (IR-SNOM), Bosn. J. Basic Med. Sci. 4 (2004) 17–21.
[175] D. Vobornik, G. Margaritondo, J.S. Sanghera, P. Thielen, I.D. Aggarwal, B. Ivanov, J.K. Miller, R. Haglund, N.H. Tolk, A. Congiu-Castellano, M.A. Rizzo, D.W. Piston, F. Somma, G. Baldacchini, F. Bonfigli, T. Marolo, F. Flora, R.M. Montereali, A. Faenov, T. Pikuz, G. Longo, V. Mussi, R. Generosi, M. Luce, P. Perfetti, A. Cricenti, Infrared near-field microscopy with the Vanderbilt free electron laser: overview and perspectives, Infrared Phys. Technol. 45 (2004) 409–416.
[176] A. Cricenti, R. Generosi, M. Luce, P. Perfetti, G. Margaritondo, D. Talley, J.S. Sanghera, I.D. Aggarwal, N.H. Tolk, A. Congiu-Castellano, M.A. Rizzo, D.W. Piston, Chemically resolved imaging of biological cells and thin films by infrared scanning near-field optical microscopy, Biophys. J. 85 (2003) 2705–2710.
[177] J. Generosi, G. Margaritondo, J.S. Sanghera, I.D. Aggarwal, N.H. Tolk, D.W. Piston, A.C. Castellano, A. Cricenti, Spectroscopic infrared near-field microscopy and X-ray reflectivity studies of order and clustering in lipid membranes, Appl. Phys. Lett. 89 (2006).
[178] J. Generosi, G. Margaritondo, J.S. Sanghera, I.D. Aggarwal, N.H. Tolk, D.W. Piston, A.C. Castellano, A. Cricenti, Infrared scanning near-field optical microscopy investigates order and clusters in model membranes, J. Microsc. (Oxford) 229 (2008) 259–263.
[179] J. Generosi, M. Kropf, G. Margaritondo, H. Hirling, S. Catsicas, K. Johnsson, N.H. Tolk, D.W. Piston, A. Cricenti, Ampa receptor imaging by infrared scanning near-field optical microscopy, Phys. Status Solidi C 5 (8) (2008) 2641–2644.
[180] J. Generosi, G. Margaritondo, M. Kropf, H. Hirling, S. Catsicas, K. Johnsson, N.H. Tolk, D.W. Piston, A. Cricenti, Photobleaching-free infrared near-field microscopy localizes molecules in neurons, J. Appl. Phys. 104 (2008).
[181] A. Dazzi, R. Prazeres, E. Glotin, J.M. Ortega, Local infrared microspectroscopy with subwavelength spatial resolution with an atomic force microscope tip used as a photothermal sensor, Opt. Lett. 30 (2005) 2388–2390.
[182] A. Dazzi, R. Prazeres, F. Glotin, J.M. Ortega, Subwavelength infrared spectromicroscopy using an AFM as a local absorption sensor, Infrared Phys. Technol. 49 (2006) 113–121.
[183] A. Dazzi, R. Prazeres, F. Glotin, J.M. Ortega, Analysis of nano-chemical mapping performed by an AFM-based ("AFMIR") acousto-optic technique, Ultramicroscopy 107 (2007) 1194–1200.
[184] A. Dazzi, F. Glotin, R. Carminati, Theory of infrared nanospectroscopy by photothermal induced resonance, J. Appl. Phys. 107 (2010).
[185] J. Houel, S. Sauvage, P. Boucaud, A. Dazzi, R. Prazeres, F. Glotin, J.M. Ortega, A. Miard, A. Lemaitre, Ultraweak-absorption microscopy of a single semiconductor quantum dot in the midinfrared range, Phys. Rev. Lett. 99 (2007).

[186] K. Kjoller, C. Prater, R. Shetty, Polymer characterization using nanoscale infrared spectroscopy, Am. Lab. 42 (2010) 20–23.
[187] B. Van Eerdenbrugh, M. Lo, K. Kjoller, C. Marcott, L.S. Taylor, Nanoscale mid-infrared evaluation of the miscibility behavior of blends of dextran or maltodextrin with poly(vinylpyrrolidone), Mol. Pharm. 9 (2012) 1459–1469.
[188] B. Van Eerdenbrugh, M. Lo, K. Kjoller, C. Marcott, L.S. Taylor, Nanoscale mid-infrared imaging of phase separation in a drug-polymer blend, J. Pharm. Sci. 101 (2012) 2066–2073.
[189] M. Lo, C. Prater, A. Dazzi, R. Shetty, K. Kjoller, Nanoscale chemical composition mapping of polymers at 100 nm spatial resolution with afm-based ir spectroscopy, Micro Nanotechnol. Sens. Syst. Appl. IV 8373 (2012).
[190] K. Kjoller, J.R. Felts, D. Cook, C.B. Prater, W.P. King, High-sensitivity nanometer-scale infrared spectroscopy using a contact mode microcantilever with an internal resonator paddle, Nanotechnology 21 (2010).
[191] J.R. Felts, K. Kjoller, M. Lo, C.B. Prater, W.P. King, Nanometer-scale infrared spectroscopy of heterogeneous polymer nanostructures fabricated by tip-based nanofabrication, ACS Nano 6 (2012) 8015–8021.
[192] M. Paulite, Z. Fakhraai, I.T.S. Li, N. Gunari, A.E. Tanur, G.C. Walker, Imaging secondary structure of individual amyloid fibrils of a beta(2)-microglobulin fragment using near-field infrared spectroscopy, J. Am. Chem. Soc. 133 (2011) 7376–7383.
[193] A. Dazzi, R. Prazeres, F. Glotin, J.M. Ortega, M. Al-Sawaftah, M. de Frutos, Chemical mapping of the distribution of viruses into infected bacteria with a photothermal method, Ultramicroscopy 108 (2008) 635–641.
[194] C. Mayet, A. Dazzi, R. Prazeres, J.M. Ortega, D. Jaillard, In situ identification and imaging of bacterial polymer nanogranules by infrared nanospectroscopy, Analyst 135 (2010) 2540–2545.
[195] C. Policar, J.B. Waern, M.A. Plamont, S. Clede, C. Mayet, R. Prazeres, J.M. Ortega, A. Vessieres, A. Dazzi, Subcellular IR imaging of a metal-carbonyl moiety using photothermally induced resonance, Angew. Chem. Int. Ed. 50 (2011) 860–864.
[196] C. Mayet, A. Dazzi, R. Prazeres, E. Allot, E. Glotin, J.M. Ortega, Sub-100 nm IR spectromicroscopy of living cells, Opt. Lett. 33 (2008) 1611–1613.
[197] T. Laredo, J.R. Dutcher, J. Lipkowski, Electric field driven changes of a gramicidin containing lipid bilayer supported on a Au(111) surface, Langmuir 27 (2011) 10072–10087.
[198] S. Shanmukh, N. Biswas, A.J. Waring, F.J. Walther, Z. Wang, Y. Chang, R.H. Notter, R.A. Dluhy, Structure and properties of phospholipid-peptide monolayers containing monomeric SP-B(1–25) ii. Peptide conformation by infrared spectroscopy, Biophys. Chem. 113 (2005) 233–244.
[199] M. Grandbois, B. Desbat, C. Salesse, Monitoring of phospholipid monolayer hydrolysis by phospholipase A2 by use of polarization-modulated Fourier transform infrared spectroscopy, Biophys. Chem. 88 (2000) 127–135.
[200] D. Kurouski, T. Deckert-Gaudig, V. Deckert, I.K. Lednev, Structure and composition of insulin fibril surfaces probed by TERS, J. Am. Chem. Soc. 134 (2012) 13323–13329.
[201] T. Deckert-Gaudig, E. Kammer, V. Deckert, Tracking of nanoscale structural variations on a single amyloid fibril with tip-enhanced Raman scattering, J. Biophotonics 5 (2012) 215–219.